AerospaceEurope Conference2021
WARSAW, POLAND | 23 -26 NOVEMBER 2021
CEAS Council of European Aerospace Societies

EVALUATION OF IMPROVED CORRECTION FACTORS FOR THE PREDICTION OF HELMHOLTZ RESONANCES

Giuseppe Catapane[1], Dario Magliacano[1], Giuseppe Petrone[1], Alessandro Casaburo[2], Francesco Franco[1] & Sergio De Rosa[1]

[1]PASTA-Lab (Laboratory for Promoting experiences in Aeronautical STructures and Acoustics), Department of Industrial Engineering - Aerospace Section, Università degli Studi di Napoli "Federico II", Via Claudio 21, 80125 Naples, Italy
[2]WaveSet S.R.L., Via A. Gramsci 15, 80122 Naples, Italy.

Abstract

Innovative meta-materials offer great flexibility for manipulating sound waves and assure unprecedented functionality in the context of acoustic applications. Indeed, they can exhibit extraordinary properties, such as broadband low-frequency absorption, excellent sound insulation, or enhanced sound transmission. More specifically, Helmholtz resonators are exploited in several applications aiming to reduce noise transmission. However, the design of acoustic meta-materials with exciting functionality still represents a challenge, therefore there is a huge interest about the conceptualization and design of innovative acoustic solutions making use of meta-material resonance effects. The main target of the present research work is to obtain an accurate prediction of the tuning frequency of a Helmholtz-resonating device, numerically modeled through a Finite Element approach. In this context, an investigation on a correction factor for the classical formulation used to estimate the Helmholtz resonance frequency starting from its geometrical characteristics, accounting for different-shaped resonators with varying neck/cavity ratios is performed. More specifically, a set of analyses are performed, and results in terms of correction factor are provided in both graphical and polynomial form, and compared with Finite Element ones, showing higher accuracy.

Keywords: acoustics, meta-material, Helmholtz, resonator

1. Introduction

It is well-known that there is an increasing growing interest on the environmental noise reduction. Aiming at this goal, different approaches could be investigated and adopted: for example, porous media, whose foam cavities dissipate the energy by viscous and thermal losses, show very good performance at high frequencies [1], while tunable acoustic devices, such as Helmholtz resonators (HRs), perform better at low frequencies.

The concept of Helmholtz resonance and the associated classical theory have been applied in the design and analysis of various systems including tuned intake manifolds of vehicles [2–4], noise attenuation in pipelines [5], attenuation of aircraft propulsor noise [6], combustion instabilities for gas-turbine engines [7]. With reference to this class of devices, Alster [8] obtained the classical formula for calculation of resonant frequencies of HRs, under the assumptions that all mass significant for oscillation of a resonator is concentrated in the neck of the resonator and that the spring constant is given by the volume of the resonator [9]. Tang et al. [10] derived the theory of a generalized HR, based on the jet-flow model that is manifested in the non-linearity of the neck flow upon the passage of a high intensity wave. Fahy et al. [11] coupled a single HR to an enclosure and tuned it to the natural frequency of one of its low order acoustic modes, also analyzing the effect on the free, and forced, vibrations of the fluid in the enclosure. Chanaud [12] developed an equation for the resonance frequency of a HR from the wave equation for the case of a cavity volume that has the shape of a rectangular parallelepiped and orifices of different geometries. de Bedout et al. [13] presented a tunable Helmholtz resonator and a feedback-based control law that achieves optimal resonator tuning for time-varying tonal noise control applications. Lei et al. [14] proposed a strategy to characterize power and ground-plane structures using a full cavity-mode frequency-domain resonator model. Griffin et al. [15] demonstrated that mechanically coupled resonators can be used for designing a particular transmission loss response, generating attenuation in a wider bandwidth, and adapting the transmission loss characteristics of a structure to attenuate disturbances at a desired frequency. Tang [16] experimentally and theoretically investigated the acoustical properties of HRs with necks having cross-section dimensions decreasing away from the entry of the resonator cavities. Park [17] introduced micro-perforated panel absorbers backed by HRs with the aim to improve sound absorption in the low-frequency range, where classical micro-perforated panel absorbers do not provide sufficient performance. HRs are analyzed by several researcher for their interesting behavior; apparently, this one does not change with the HR shape. Nevertheless, resonance frequency prediction formulas are not so much faithful for shapes that are different respect to the typical analyzed in literature (like cylinder neck - cylinder cavity); furthermore, a classic geometry like cylinder neck - cylinder cavity can have resonance frequency shift for different radius ratios. The scope of this paper is to obtain an accurate prediction of the tuning frequency of a HR device, for several combination of neck-cavity geometries.

The present work is structured as follows: in Section 2., the methodologies and objectives are presented, together with some details about geometrical properties (Section 2.1) and Finite Element (FE) implementation (Section 2.2) of the analyzed configurations. Successively, in Section 3., some analyses for different neck/cavity ratios and geometries are performed, and some results in terms of correction factor (Section 3.1), resonance frequency (Section 3.2) and absolute errors (Section 3.3) are provided and discussed. In conclusion, in Section 4., the main achievements of the present research are summarized and some possible future expansions are identified.

2. Definition of the problem

In this section, Helmholtz resonators are numerically modeled and studied, accounting for different shapes with varying neck/cavity ratios.

A Helmholtz resonator (HR) is a tunable device with rigid walls and filled of fluid, whose geometry is usually represented by a neck followed by a cavity. With reference to acoustic applications, HRs exhibit a single resonance frequency; thus, they are commonly defined as 1-Degree-of-Freedom (DoF) systems. Indeed, HRs may be conceptually assimilated to a mass-spring system, in which the fluid in the neck represents the mass $m = \rho_0 S_{neck} l_{neck}$, while the volume acts as a spring with stiffness $K = \rho_0 c_0^2 S_{neck}^2 / V_{cavity}$, where: ρ_0 is the density of the fluid, c_0 is the speed of sound in the fluid, S_{neck} is the area of the section of the neck, V_{cavity} is the volume of the cavity, and l_{neck} is the main length of the neck.

A first attempt of obtaining an approximate mathematical estimation of a HR tuning frequency f_{HR}, starting from its fundamental geometrical characteristics, was proposed by Rayleigh [18] as:

$$f_{HR} = \frac{c_0}{2\pi} \sqrt{\frac{S_{neck}}{V_{cavity}(l_{neck} + \frac{4}{3\pi} d_{neck})}} \tag{1}$$

where $(4/3\pi) d_{neck}$ is the end-correction factor proposed by Rayleigh for accounting neck-cavity junction effects due to an abrupt change between the circular cross sections. This change leads to an additional impedance, defined as discontinuity inductance.

The physical phenomenon is well explained by Karal [19], who relates the discontinuity inductance to the ratio between the tube radii. This additional impedance can be conceptually interpreted as an increase in the length of the tube; moreover, if the ratio of the tube radii is unitary, the circular section is unchanged and thus the length does not need any corrections; on the other hand, for a ratio equal to zero (an open tube fitted with an infinite flange), the correction factor corresponds to the Rayleigh's one. Thus, it is logical that Rayleigh's correction works well for low value of tube radii ratio, while it needs other considerations when the ratio is increasing. Successively, Ingard [20] modified Rayleigh's formula by increasing its complexity in order to provide an alternative estimation of HR

frequency, which has explicit dependence on the ratio ξ between the representative lengths in the section plane of the neck and the cavity, respectively labeled as d_{neck} and d_{cavity}. Ingard developed this approach for three geometrical configurations (cylindrical neck and cylindrical cavity, cylindrical neck and parallelepiped cavity, parallelepiped neck and parallelepiped cavity).
Analogously to Ingard's approach, also Rayleigh's formula can be written by outlining its dependence from ξ, in the form of:

$$f_{HR} = \frac{c_0}{2\pi}\sqrt{\frac{S_{neck}}{V_{cavity} l_{neck}(1+\frac{4}{3\pi}\frac{d_{cavity}}{l_{neck}}\xi)}} \tag{2}$$

Finite Elements results demonstrate how Rayleigh's and Ingard's estimations perform well in a limited range of ξ, while sensibly differing from FE results for values of ξ outside of it. Thus, a new empirical prediction of HR frequency is developed herein, with the aim of obtaining a more accurate evaluation compared with those already available in the relevant literature. This is done starting from Eq. (2), and investigating the correction factor c_f, which plays the role defined as follows:

$$f_{HR} = \frac{c_0}{2\pi}\sqrt{\frac{S_{neck}}{V_{cavity} l_{neck}(1+c_f\xi)}} \tag{3}$$

2.1 Geometrical properties

Six different geometrical configurations are considered herein. A summary of the studied configurations is reported in Table 1, the same being also shown in Figure 1. Moreover, a precise explanation of the characteristic lengths of necks and cavities for the studied configurations are reported in Table 2. It should be clarified that the equivalent edge of the parallelepiped section is obtained by computing the square root of the product between the two edge lengths of the parallelepiped section itself.

Table 1 – Geometrical description of the studied configurations.

Configuration	**Neck shape**	**Cavity shape**
1	Cylinder	Cylinder
2	Parallelepiped	Cylinder
3	Cylinder	Parallelepiped
4	Parallelepiped	Parallelepiped
5	Cylinder	Sphere
6	Parallelepiped	Sphere

Table 2 – Characteristic lengths of necks and cavities for six different geometrical configurations, where $\xi = d_{neck}/d_{cavity}$.

Configuration	d_{neck}	d_{cavity}
1	Diameter of the cylinder	Diameter of the cylinder
2	Equivalent edge of the parallelepiped section	Diameter of the cylinder
3	Diameter of the cylinder	Equivalent edge of the parallelepiped section
4	Equivalent edge of the parallelepiped section	Equivalent edge of the parallelepiped section
1	Diameter of the cylinder	Diameter of the sphere
6	Equivalent edge of the parallelepiped section	Diameter of the sphere

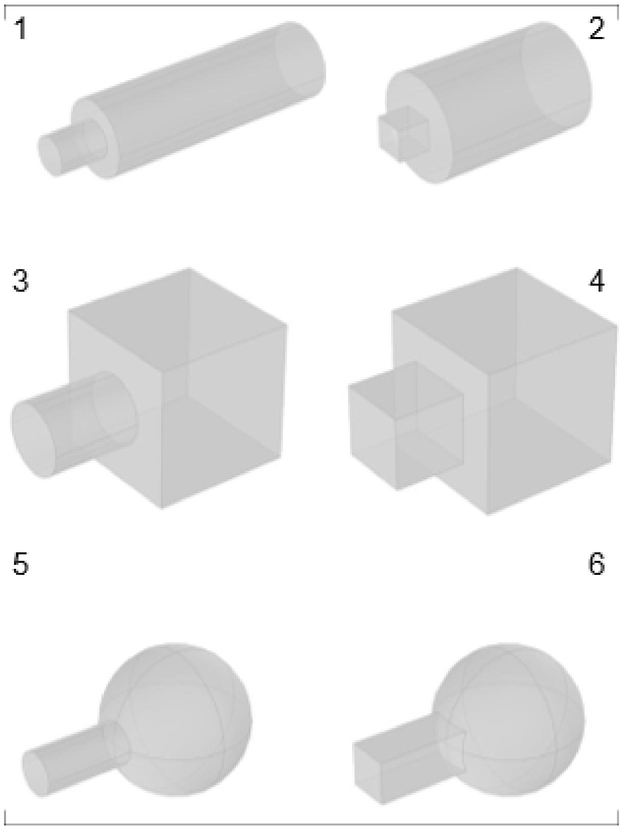

Figure 1 – Representation of the studied configurations, numbered as indicated in Table 1.

2.2 Finite Element implementation

For what concerns the FE implementation, the module "Pressure Acoustics and Frequency Domain" of COMSOL MultiPhysics is used both as modeling tool and numerical solver. For all configurations presented in this work, the mesh consists of tetrahedral elements generated through physics-controlled algorithms that are pre-implemented in the software. Nevertheless, the authors verified that the maximum element size of each HR meshed is always lower then $1/4$ of the minimum wavelength λ. In Table 3, the average number of FE mesh elements for each of the studied configurations are reported.

Table 3 – Average number of FE mesh elements.

Configuration	Domain	Boundary	Edge
1	5652	1130	149
2	3021	682	114
3	5846	985	127
4	6731	1044	133
5	2828	656	116
6	3007	702	125

The analyzed HRs are filled by air, whose properties are: density $\rho_0 = 1.225$ [kg/m^3], speed of sound $c_0 = 343$ [m/s]. The analyses are carried out considering an excitation consisting of a unit pressure boundary condition applied to the free end of the neck, while the HR walls are modeled through Sound Hard Boundary Wall (SHBW) conditions, which means that the normal component of the acceleration (and thus the velocity) is zero. A detailed description of classical FE formulation and equations can be easily found in the context of the relevant literature [21].

3. Analyses and results for different neck/cavity ratios and geometries

In this section, the six configurations previously defined are studied, and some results are presented as functions of the ratio ξ. The dimensions of HRs are chosen in order to be sufficiently big to avoid manufacturing issues, while also being sufficiently small to preserve their interest in terms of acoustic applicability in the fields of transport engineering (e.g.: aerospace, automotive, etc.). More specifically, the neck dimensions are of the order of $2 \div 10$mm, while the cavity dimension is varying from 2 to 100mm.

3.1 Graphical estimation of the correction factor for an improved predictive formula

First, a FE parametric test campaign, as a function of the ratio ξ, is carried out with the aim to estimate the resonance frequency of HRs that represent Configurations 1-6. Starting from this set of data, Eq. 3 is inverted to obtain the value of the correction factor c_f as:

$$c_f = \left(\frac{c_0^2}{4\pi^2}\frac{S_{neck}}{f_{HR}^2 V_{cavity} l_{neck}} - 1\right)\xi^{-1} \tag{4}$$

Such values of the correction factor are shown in Fig. 2. It may be interesting to notice that, for all the analyzed configurations, in the range $0.05 < \xi < 0.3$ the values of c_f sharply change, while varying in a much smoother manner in the range $0.3 < \xi < 0.95$, where they are always bounded between $c_f = 0.5$ and $c_f = 2.5$. These results may be intended as a carpet plot, in which the potential user may enter with a designed value of ξ, choose the appropriate curve according to the considered geometry, and obtain a value of c_f that can be used in Eq. 3 in order to predict the resonance frequency of a specific HR device. It should be noted that the analyzed configurations do not represent the only solutions for Helmholtz Resonator geometry, but they are the most used for the acoustic applications; then, neck or cavity geometries that are different from these configurations have to be developed with a new numerical campaign. Nevertheless, the approach for new numerical tests can be unchanged.

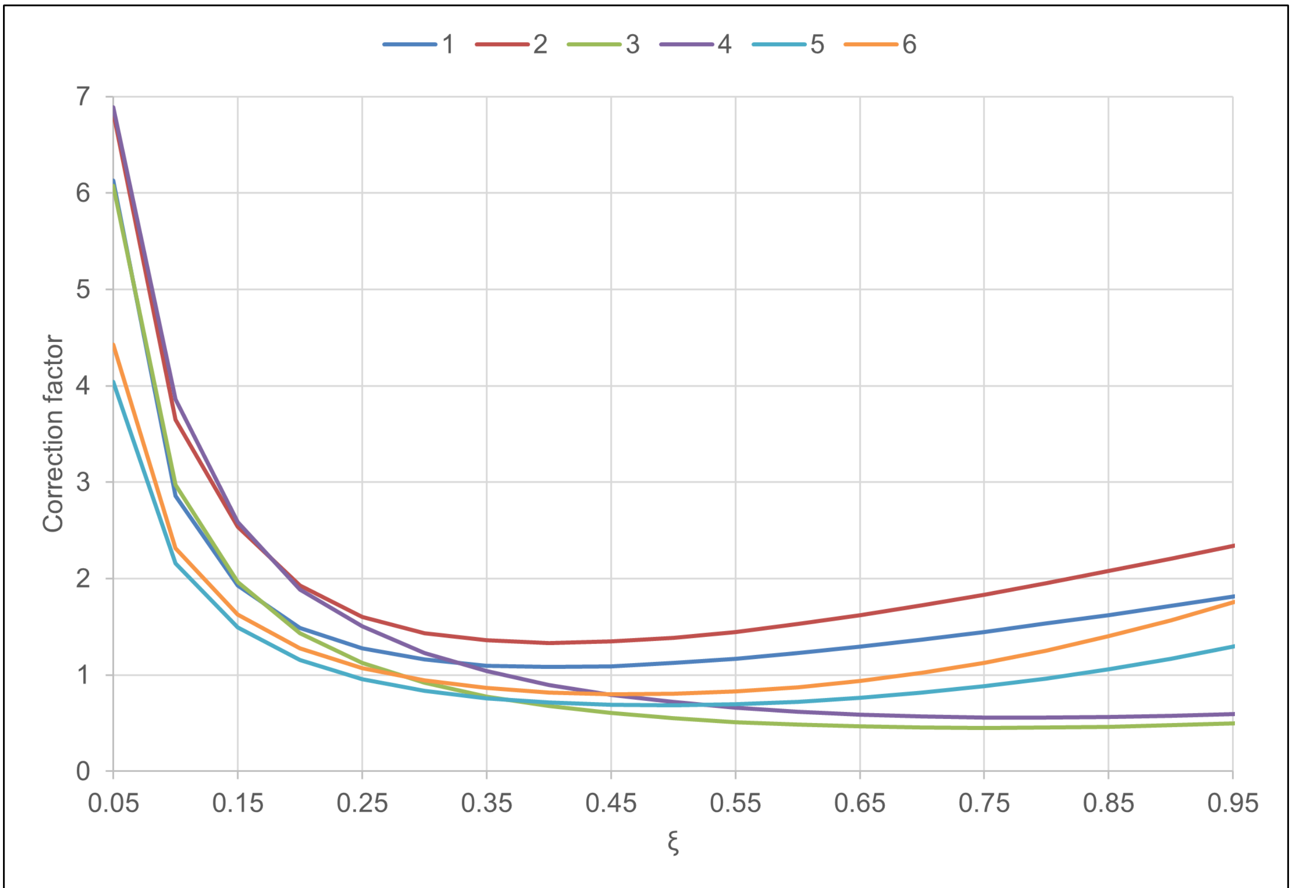

Figure 2 – FE estimation of the correction factor for the six studied HR configurations, as functions of ξ.

3.2 Calculation of Helmholtz resonance frequency through Rayleigh's formula, Finite Element computation and polynomial approximation

With the objective of developing an alternative approach to the graphical estimation of the correction factor c_f, and consequently of the HR frequency f_{HR}, described in Section 3.1, a 3rd-order polynomial approximation of the correction factors is proposed herein. Since Rayleigh's formula reported in Eq. (2) performs for ratios $0.05 < \xi < 0.3$ with a level of accuracy that is definitely acceptable, and considering that, as already underlined, in the range $0.05 < \xi < 0.3$ the values of c_f vary meaningfully, while changing less in the range $0.3 < \xi < 0.95$, then it may be convenient to directly rely on Eq. (2) up to $\xi = 0.3$, and to contextually develop a polynomial approximation for higher values of ξ.

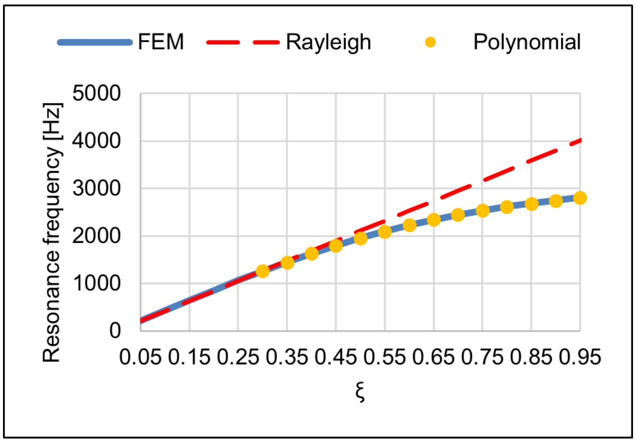

(a) Configuration 1

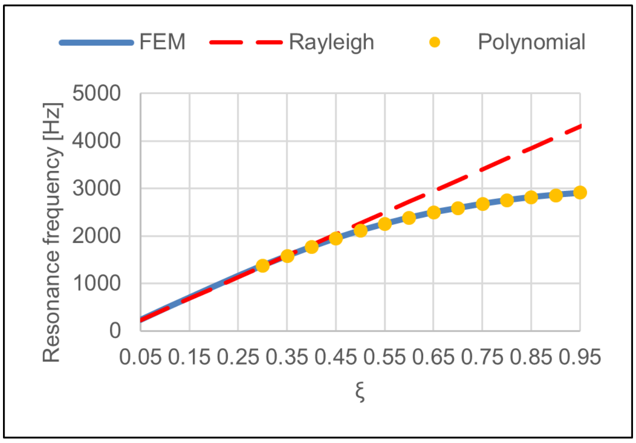

(b) Configuration 2

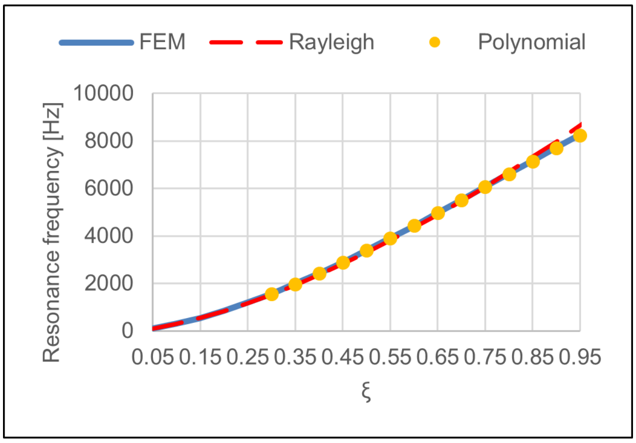

(c) Configuration 3

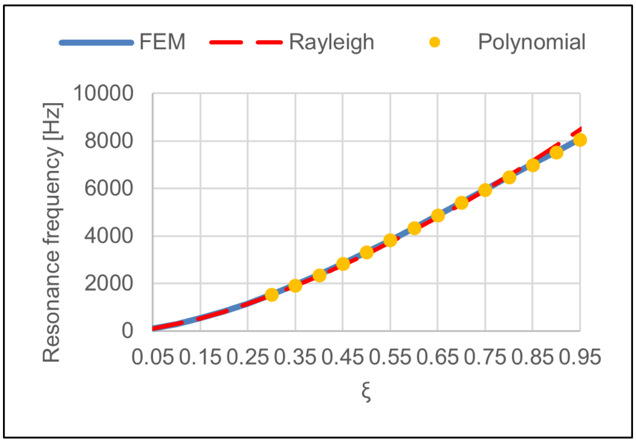

(d) Configuration 4

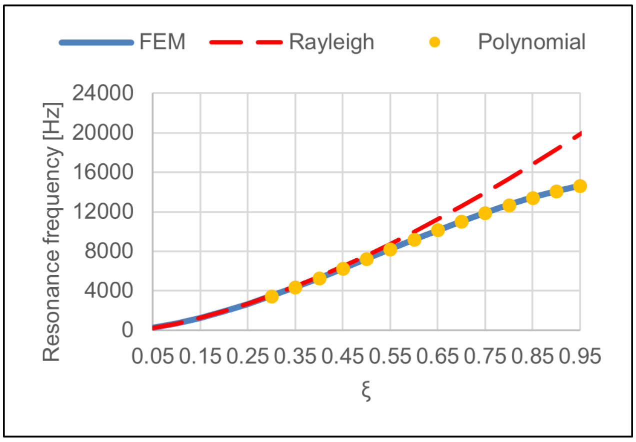

(e) Configuration 5

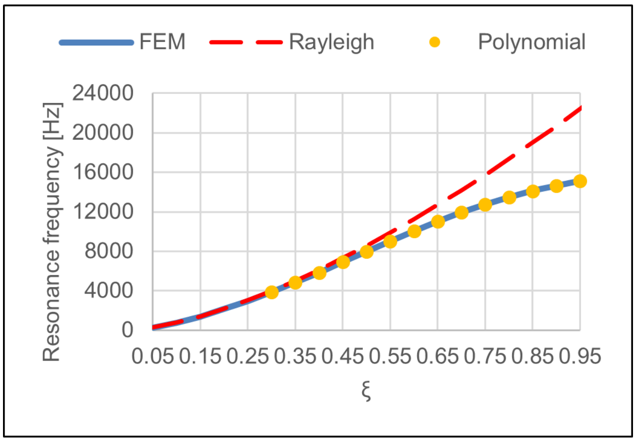

(f) Configuration 6

Figure 3 – Comparison of Helmholtz resonance frequency estimations for each analyzed configuration.

As it may be noticed from Figure 3, which show the HR frequencies of the six studied configurations, for $0.05 < \xi < 0.3$ Rayleigh's formula is always able to catch the FE behavior with a negligible accuracy error, while for $\xi > 0.3$ the proposed 3rd-order polynomial approximations almost perfectly follow FE values. Clearly, if one wanted to derive a polynomial expression with reasonable validity in the whole ξ range, a higher-order polynomial would have been needed. The above-mentioned polynomial expressions are derived using MATLAB's built-in "polyfit" function and are meant to be used in Eq. (3) with the aim of mathematically calculating the resonance frequency of a HR. The expressions that refer to Configurations from 1 to 6 are reported in Eqs. (5)-(10), respectively.

$$c_{f1} = -3.72\xi^3 + 9.31\xi^2 - 5.89\xi + 2.21 \tag{5}$$

$$c_{f2} = -5.16\xi^3 + 12.9\xi^2 - 8.20\xi + 2.89 \tag{6}$$

$$c_{f3} = -3.42\xi^3 + 8.83\xi^2 - 7.34\xi + 2.43 \tag{7}$$

$$c_{f4} = -4.61\xi^3 + 11.8\xi^2 - 9.91\xi + 3.28 \tag{8}$$

$$c_{f5} = -1.27\xi^3 + 5.60\xi^2 - 4.69\xi + 1.78 \tag{9}$$

$$c_{f6} = -1.08\xi^3 + 6.33\xi^2 - 5.31\xi + 2.00 \tag{10}$$

3.3 Evaluation of the relative errors of Rayleigh's formula and of the proposed approach with reference to Finite Element results

Finally, in this section, the relative errors of Rayleigh's formula and of calculated polynomial expressions are provided, considering FE results as the reference ones. In detail, in Figure 4 it may be seen that, for $\xi < 0.3$, the relative error of Rayleigh's formula respect to FE data is always lower than 3%, while increasing up to 50% for higher values of ξ in the case of some of the studied configurations.

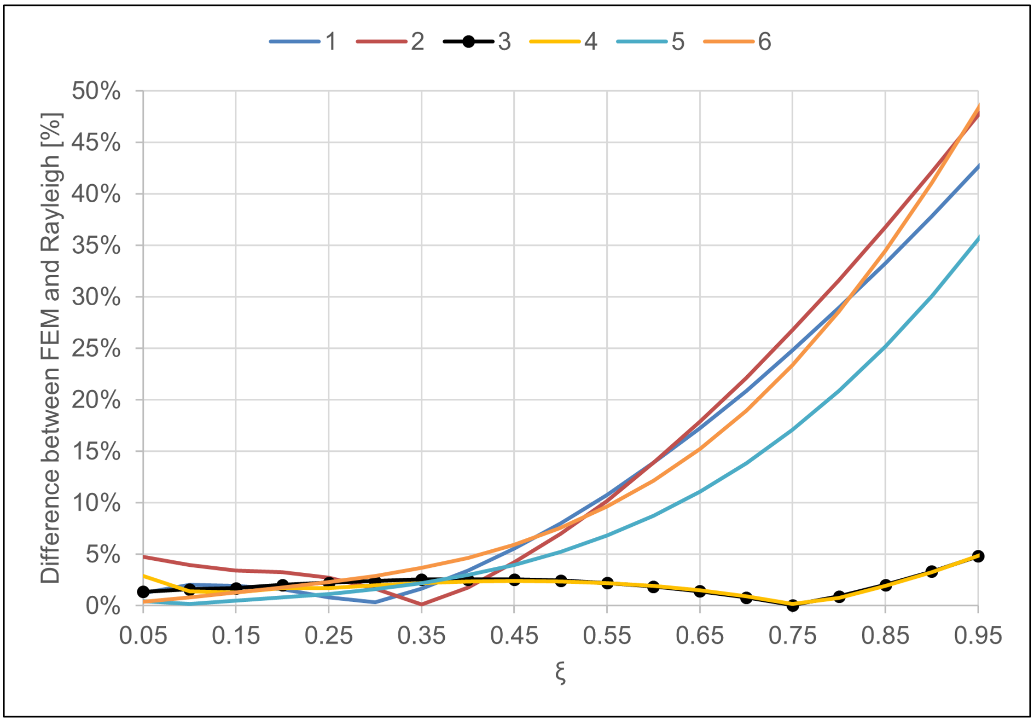

Figure 4 – Evaluation of the relative errors of Rayleigh's formula, with reference to Finite Element results, for the six studied HR configurations, as functions of ξ.

Moreover, for Configurations 3 and 4, errors are quite similar and, in general, lower than 5% in the whole ξ range; according to the desired accuracy, this may allow the usage of Eq. 2 when having a HR with a parallelepiped cavity, regardless of the value of ξ. For what concerns the relative difference between the HR frequency predictions obtained making use of Eqs. (5)-(10), and the HR frequencies got with the numerical campaigns, it is lower than 0.5% in the entire ξ range, thus eventually representing a valid alternative approach compared to the graphical one introduced and discussed in Section 3.1.

4. Conclusions

The present work aims at obtaining an accurate prediction of the tuning frequency of Helmholtz-resonating devices. To this scope, it is performed an investigation on a correction factor for the classical formulation used to estimate the Helmholtz resonance frequency starting from its geometrical characteristics, in the case of different-shaped resonators with varying neck/cavity ratios. In detail, a set of analyses are carried out, and results in terms of correction factor are provided in both graphical and polynomial form, also demonstrating their good accuracy respect to Finite Element ones. The methodologies and objectives of this work have been presented, together with some details about geometrical properties and FE implementation of the analyzed configurations; then, some analyses for different neck/cavity ratios and geometries have been performed, and the related results in terms of correction factor, resonance frequency and absolute errors are provided and discussed.

A possible extension of the work presented herein may be constituted by an experimental validation of FE results. Furthermore, the scalability of results found in this context should be verified too, to assure their applicability on structures with very different sizes respect to those considered herein. In addition, the effect on Helmholtz resonance frequency and amplitude due to the presence of a wall material may be investigated too.

Acknowledgements

The authors acknowledge the support of the Italian Ministry of Education, University and Research (MIUR) through the project DEVISU, funded under the scheme PRIN-2107 – grant agreement No. 22017ZX9X4K006.

Contact Author Email Address

g.catapane@studenti.unina.it

References

[1] D. Magliacano, M. Ouisse, S. De Rosa, F. Franco, and A. Khelif, “Computation of acoustic properties and design guidelines of periodic Biot-modeled foams”, Applied Acoustics, vol. 168, p. 107428, 2020, doi: 10.1016/j.apacoust.2020.107428.

[2] M. P. Thompson and H. W. Engleman, “The two types of resonance in intake tuning”, American Society of Mechanical Engineers, 1969.

[3] M. R. Driels, “Dynamics of I. C. Engine induction systems”, Journal of Sound and Vibration, vol. 43, no. 3, pp. 499–510, Dec. 1975, doi: 10.1016/0022-460X(75)90003-6

[4] R. T. Jameson and P. A. Hodgins, “Improvement of the torque characteristics of a small, high-speed engine through the design of Helmholtz-tuned manifolding”, Feb. 1990. doi: 10.4271/900680.

[5] M. Farooqui, S. Mekid, M. Hawwa, and S. Mekid, “Design of Helmholtz Resonators in one and two degrees of freedom for noise attenuation in pipelines.”, 2011.

[6] L. J. Gorny, G. H. Koopmann, W. Neise, and O. Lemke, “Attenuation of Ducted Axial Propulsors’ Blade Tone Noise Using Adaptively Tunable Resonators”, 2007.

[7] D. Zhao and A. S. Morgans, “Tuned passive control of combustion instabilities using multiple Helmholtz resonators”, Journal of Sound and Vibration, vol. 320, no. 4–5, pp. 744–757, Mar. 2009, doi: 10.1016/j.jsv.2008.09.006.

[8] M. Alster, “Improved calculation of resonant frequencies of Helmholtz resonators”, Journal of Sound and Vibration, vol. 24, no. 1, pp. 63–85, 1972, doi: 10.1016/0022-460X(72)90123-X.

[9] L. Kinsler, A. Frey, A. Coppens, and Sanders. James, Fundamental of Acoustics. 1922.

[10] P. K. Tang and W. A. Sirignano, “Theory of a generalized Helmholtz resonator”, Journal of Sound and Vibration, vol. 26, no. 2, pp. 247–262, 1973, doi: 10.1016/S0022-460X(73)80234-2.

[11] F. J. Fahy and C. Schofield, “A note on the interaction between a Helmholtz resonator and an acoustic mode of an enclosure”, Journal of Sound and Vibration, vol. 72, no. 3, pp. 365–378, 1980, doi: 10.1016/0022-460X(80)90383-1.

[12] R. C. Chanaud, “Effects of geometry on the resonance frequency of Helmholtz resonators”, Journal of Sound and Vibration, vol. 178, no. 3. pp. 337–348, 1994. doi: 10.1006/jsvi.1994.1490.

[13] J. M. De Bedout, M. A. Franchek, R. J. Bernhard, and L. Mongeau, “Adaptive-passive noise control with self-tuning Helmholtz resonators”, Journal of Sound and Vibration, vol. 202, no. 1, pp. 109–123, 1997, doi: 10.1006/jsvi.1996.0796.

[14] G. T. Lei, R. W. Techentin, and B. K. Gilbert, “High-frequency characterization of power/ground-plane structures”, IEEE Transactions on Microwave Theory and Techniques, vol. 47, no. 5, pp. 562–569, 1999, doi: 10.1109/22.763156.

[15] S. Griffin, S. A. Lane, and S. Huybrechts, “Coupled helmholtz resonators for acoustic attenuation”, Journal of Vibration and Acoustics, Transactions of the ASME, vol. 123, no. 1, pp. 11–17, 2001, doi: 10.1115/1.1320812.

[16] S. K. Tang, “On Helmholtz resonators with tapered necks”, Journal of Sound and Vibration, vol. 279, no. 3–5, pp. 1085–1096, 2005, doi: 10.1016/j.jsv.2003.11.032.

[17] S. H. Park, “Acoustic properties of micro-perforated panel absorbers backed by Helmholtz resonators for the improvement of low-frequency sound absorption”, Journal of Sound and Vibration, vol. 332, no. 20, pp. 4895–4911, 2013, doi: 10.1016/j.jsv.2013.04.029.

[18] J. W. S. Rayleigh, The Theory of Sound. 1898. doi: 10.1038/058121a0.

[19] F. C. Karal, “The Analogous Acoustical Impedance for Discontinuities and Constrictions of Circular Cross Section”, THE JOURNAL OF THE ACOUSTICAL SOCIETY OF AMERICA, vol. 25, 1953.

[20] U. Ingard, “On the theory and design of acoustic resonators”, The Journal of the Acoustical Society of America, vol. 25, no. 6, pp. 1037–1061, 1953.

[21] Isaac C.W., Wrona S., Pawelczyk M., and Roozen N.B., “Numerical investigation of the vibro-acoustic response of functionally graded lightweight square panel at low and mid-frequency regions”, Composite Structures, vol. 259, 2021, doi: 10.1016/j.compstruct.2020.113460.